

An Efficient Compensation Algorithm for Current Transformer Saturation Effects

Jiuping Pan, *Member, IEEE*, Khoi Vu, *Member, IEEE*, and Yi Hu, *Member, IEEE*

Abstract—Current transformer (CT) saturation leads to inaccurate current measurement and, therefore, may cause malfunction of protective relays and control devices that use currents as input signals. This paper introduces an efficient compensation algorithm capable of converting from a sampled current waveform that is distorted by CT saturation to a compensated current waveform. Attractive features include quick response time, no cumulative estimation errors, desired sample-by-sample output, independent of CT parameters/characteristics and secondary burdens, and simplicity for online implementation. The accuracy and robustness of the introduced compensation algorithm are demonstrated through extensive test cases reflecting a wide range of variations in fault conditions and CT parameters.

Index Terms—Control and protection, current transformer (CT), power systems, saturation effects, waveform compensation.

I. BACKGROUND

THE MEASURE of current transformer (CT) performance is the ability to reproduce accurately the primary current on the secondary side of the CT in terms of its magnitude and shape. Fault currents, which may be much greater than rated currents and which may be nonsymmetrical, often cause distortion of the secondary current due to CT saturation effects. CT saturation leads to inaccurate current measurement and, therefore, may cause malfunction of protective relays and control devices that use currents as input signals. For example, a distorted current waveform may result in delayed operation of inverse-time overcurrent relays due to underestimation of the root-mean-square (rms) value of current waveforms. Distance relays may experience both over-reach and under-reach problems in fault impedance calculations due to inaccurate current phasor measurement.

One approach of reducing the impact of CT saturation is to use waveform compensation or restructuring algorithms that attempt to reconstruct the secondary current waveform. The method proposed in [1] requires that a function be developed based on given CT parameters to approximately represent the nonlinear core characteristics of a specific model of CT. In another method [2], an artificial neural network (ANN) attempts to learn the nonlinear characteristics of CT magnetization and restructures the waveform based on the learned characteristics. However, these methods could not be universally applied to

different CTs because CT saturation effects vary from CT to CT even for CTs of the same type. This is due to the variations of actual CT saturation characteristics and mainly the secondary burdens [e.g., volt-ampere (VA) loading and power factor] that a CT carries.

Another approach of reducing the impact of CT saturation is to apply variable data window protection and control algorithms that only use the measured currents during the periods when the CTs are not saturated [3], [4]. This approach must use a saturation detection technique to identify the unsaturated waveform portions from a partially distorted fault current waveform and specialized protection/control algorithms that can operate on a variable data window shorter than a full cycle. However, the performance of existing saturation detection techniques will generally not be reliable when the CT secondary burden contains a significant inductive component.

Reference [5] disclosed a method for obtaining an undistorted version of a fault current waveform suffering from saturation distortion. The method first performs a screening process throughout the recorded fault current waveform to determine unsaturated portions of the partially distorted waveform. Then, a digital representation of the fault current waveform is obtained using the identified unsaturated data blocks. Finally, a reconstructed waveform is formed by replacing the saturated portions of the partially distorted waveform with the data points calculated from the digital representation. This method is a good solution for offline waveform reconstruction where the fault currents are recorded for the entire waveform and reconstruction occurs at a later time. However, it is not suitable for applications relating to online protection and control devices/apparatus used in power systems where a decision must be made as fast as possible, generally within a few cycles after fault inception.

In addition to the above methods, some other specific measures have been used for protection and control functions in power systems. These include using harmonic contents in saturated current waveform as restraining quantity, or using current sum as restraining quantity in differential protection, etc. In some other applications, saturation detection techniques have been used to block and unblock the operation of certain protection/control functions. The main drawbacks of these methods are delayed operation or reduced sensitivity.

This paper introduces an efficient CT saturation compensation algorithm that can significantly reduce the errors in measured current waveform caused by CT saturation effects. The compensation algorithm is capable of converting from a sampled current waveform that is distorted by CT saturation effects to a compensated current waveform. As will be shown, attractive features of this compensation algorithm include quick response

Manuscript received February 11, 2003; revised April 22, 2003. Paper no. TPWRD-00059-2003.

The authors are with the ABB Corporate Research, Raleigh, NC 27606 USA (e-mail: jiuping.pan@us.abb.com; khoi.vu@us.abb.com; yhu101@hotmail.com).

Digital Object Identifier 10.1109/TPWRD.2004.835273

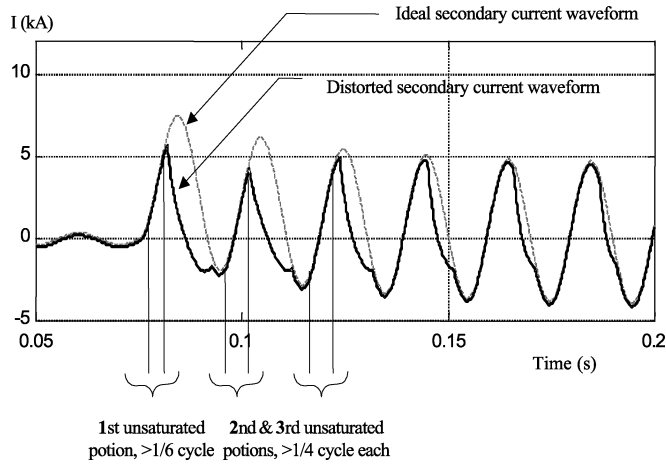


Fig. 1. Ideal and saturated CT secondary current waveforms.

time, no cumulative estimation errors, independent of CT parameters/characteristics and secondary burdens, and simplicity for online implementation.

The remainder of this paper is organized as follows. Section II provides a description of the methodology. Section III shows how the proposed algorithm can be implemented for power system protection and control applications. Section IV presents the results of performance evaluation regarding the algorithm robustness and accuracy under various fault conditions and CT parameters. Concluding remarks are given in Section V.

II. METHODOLOGY DESCRIPTION

CT performance requirements under steady-state and symmetrical fault conditions are specified in IEEE standard C57.13-1993 [6]. Proper selection of CT ratios will assume acceptable measurement errors (i.e., the standard 10% CT error) for steady-state and symmetrical faults up to 20 times the rated CT primary currents. However, faults in power system very often involve a dc offset superimposed on the symmetrical component in one or more of the three-phase currents, resulting in CT saturation at much lower current levels than symmetrical currents without dc offset. It is well known that a partially distorted CT secondary current waveform due to saturation contains two distinguished portions within each cycle—a saturated waveform portion and an unsaturated waveform portion. The waveform is not saturated at least for about 1/6 cycle before the first saturated waveform portion and about 1/4 cycle between any two successive saturated waveform portions as shown in Fig. 1.

Additionally, starting from the second unsaturated waveform portion, there exist unsaturated points that occur exactly one cycle later as compared to the previous unsaturated waveform portion. The unsaturated waveform portions can be determined by using a reference point (RP), which can be determined shortly after the fault inception. The reference point is defined as the first fault current data sample after waveform zero crossing into the cycle portion of a fault current waveform in the same direction of dc offset. Criteria used for determining an RP are discussed as follows.

A sample I_N [i.e., I-sample(N)] is determined as the RP if the samples thereafter within a range of no less than a predefined

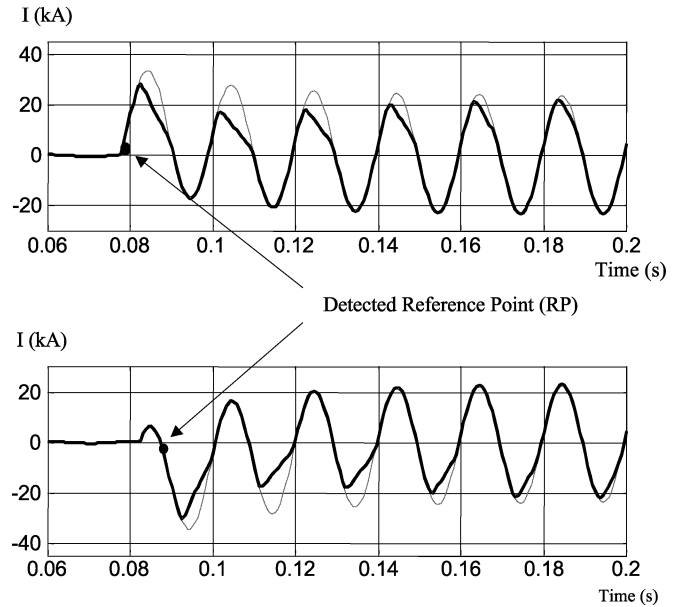


Fig. 2. Ideal and saturated CT secondary current waveforms with reference points indicated.

portion, say M samples, of a cycle relative to sample I_N , satisfy both condition (a) and condition (b)

- (a) $|I_N| > K|I_{rated}|$
- (b) $|I_{m+1}| > K_m|I_m|$ ($m = N, N+1, \dots, N+M-1$)

where I_{rated} is the rated CT primary current, K and K_m ($m = N, N+1, \dots, N+M-1$) are a set of predefined parameters.

When the measurement exceeds the preset threshold, that is both condition (a) and condition (b) are satisfied, the first sample of all samples used in the set RP criterion is saved as the RP. Typically, the predefined portion of a cycle for detecting an RP is about 1/8 cycle (or about 45°), and parameters K and K_m can be selected based on the magnitude ratio of two adjacent samples during a predefined portion of a cycle, from about the first 1/8 to 1/6 cycle of a standard sinusoidal waveform. An example of a typical value for K would be 1.2 and typical values for K_1 , K_2 , and K_3 would be 1.5, 1.35, and 1.25. Fig. 2 shows illustrative examples of detected RP points in two different fault conditions. In one fault condition, the dc offset is positive and the RP occurs after the first zero crossing into positive current. In the second fault condition, the dc offset is negative and the RP occurs after the first zero crossing into negative current.

After setting the RP, the sampled waveform can then be separated into two portions—an unsaturated waveform portion and a saturated waveform portion. The unsaturated waveform portion contains samples in a continuous data block that are unsaturated. The saturated waveform portion between two adjacent unsaturated waveform portions contains samples also in a continuous data block that may be saturated. The first unsaturated waveform portion is the one that includes the RP while the second unsaturated waveform portion contains the sample that is one cycle apart from the RP. The same allocation procedure follows thereafter for the succeeding unsaturated waveform portions such that each of them contains the sample that is apart from the RP by one more cycle as compared to the previous unsaturated waveform portion. In general, the unsaturated

waveform portion is about 1/6 to 1/4 cycle and it may or may not be symmetrical to the RP or the sample apart from the RP by an integer number of cycles.

To estimate I-compensated, it is noted that a fault current can be expressed as a combination of two components. The first component is a periodic and steady-state component determined by the source voltage and fault circuit impedance. The second component is a transient dc offset component produced at the fault instant against the sudden current changes. This dc offset component will then disappear by decaying according to the L/R time constant of the power system.

Accordingly, the following equation should be satisfied for any unsaturated data point I_k measured from a fault current waveform:

$$I_k = A \cos \left(2\pi k \frac{f}{f_{\text{samp}}} + \varphi \right) + B e^{\lambda k} \quad (1)$$

where f_{samp} denotes the sampling frequency of data-acquisition module, and f is the power-line frequency. The unknown parameters are A , B , φ , and λ .

Theoretically, knowing these four unknown parameters will define the entire fault current waveform and, therefore, can be used to estimate the saturated portion of the waveform. Numerical values for A , B , φ , and λ can be properly estimated using the least-squares (LS) curve fitting method if adequate samples can be obtained from unsaturated waveform portions.

Equation (1) can be reformulated as (2) by expanding the cosine term and taking the first-order approximation of the Taylor series for the exponential function

$$I_k = (A \cos \varphi) \cos \omega k + (-A \sin \varphi) \sin \omega k + B + \lambda k. \quad (2)$$

Equation (2) can be rewritten as (3) after using parameters C_1 and C_2 to replace $(A \cos \varphi)$ and $(-A \sin \varphi)$ and using angular frequency ω to represent $2\pi * f/f_{\text{samp}}$, respectively

$$I_k = C_1 \cos \omega k + C_2 \sin \omega k + B + \lambda k. \quad (3)$$

Equation (4) is formulated with samples from two previous consecutive unsaturated waveform portions

$$\begin{bmatrix} \cos \omega(k_i) & \sin \omega(k_i) & k_i & 1 \\ \dots & \dots & \dots & \dots \\ \dots & \dots & \dots & \dots \\ \cos \omega(k_i + m_i) & \sin \omega(k_i + m_i) & k_i + m_i & 1 \\ \dots & \dots & \dots & \dots \\ \dots & \dots & \dots & \dots \\ \cos \omega(k_j) & \sin \omega(k_j) & k_j & 1 \\ \dots & \dots & \dots & \dots \\ \dots & \dots & \dots & \dots \\ \cos \omega(k_j + m_j) & \sin \omega(k_j + m_j) & k_j + m_j & 1 \end{bmatrix} \times \begin{bmatrix} C_1 \\ C_2 \\ \lambda \\ B \end{bmatrix} = \begin{bmatrix} I(k_i) \\ \dots \\ \dots \\ I(k_i + m_i) \\ \dots \\ \dots \\ I(k_j) \\ \dots \\ \dots \\ I(k_j + m_j) \end{bmatrix}. \quad (4)$$

In (4), the samples obtained from the first unsaturated waveform portion are numbered k_i to $k_i + m_i$ and the samples obtained

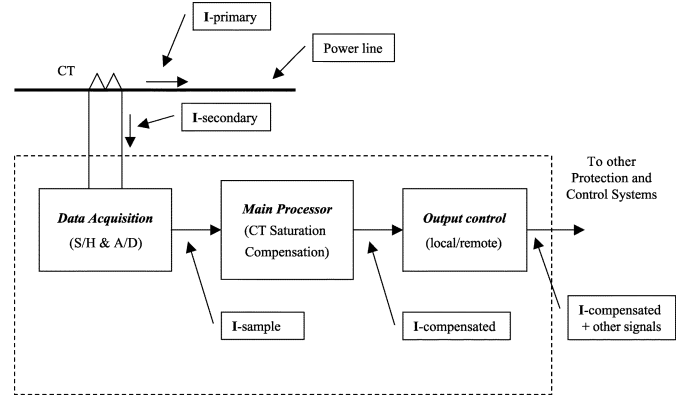


Fig. 3. Online CT saturation compensation system.

from the second unsaturated waveform portion are numbered k_j to $k_j + m_j$, respectively.

A concise matrix representation of (4) is given in (5) from which (6) can be derived for estimating the samples of the incoming saturated waveform portion immediately after the second unsaturated waveform portion and where T represents matrix transpose operator

$$\mathbf{MP} = \mathbf{I} \quad (5)$$

$$\mathbf{P} = (\mathbf{M}^T \mathbf{M})^{-1} \mathbf{M}^T \mathbf{I}. \quad (6)$$

Once the parameters A , B , φ , and λ are determined, those possibly saturated samples can then be replaced with the model outputs.

Flexibility is allowed in formulating the above described compensation algorithm. Compensation based on data samples in two previous consecutive unsaturated waveform portions to estimate I-compensated, either using all of the samples of the two stored portions or using only a part of the samples in the two stored portions, can meet response and accuracy requirements of most protection and control applications in power systems. To achieve even fast response, the compensation of the first saturated portion may use samples in only the first unsaturated waveform portions. On the other hand, for more accurate fault current waveform restructuring, more than two previous consecutive unsaturated waveform portions can be used.

III. SYSTEM IMPLEMENTATION

The above described compensation algorithm may be implemented for various online protection and control applications in power systems. Fig. 3 is a block diagram showing how the introduced method can be implemented for online compensation of current transformer saturation. A sampling rate of 32 samples or higher per cycle is assumed in a data-acquisition module. Fig. 4 is a flowchart illustrating the operation process of the online CT saturation compensation from receiving a data sample to generating a compensated sample if the sample is determined as within a saturated portion of fault current waveform.

As shown in Fig. 4, for each received current data sample, the system determines whether an RP has been set. If an RP has not been set, the system simply saves the received sample

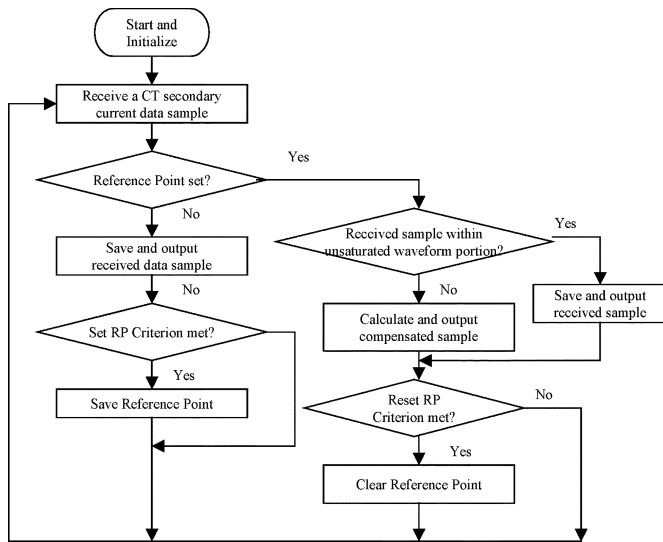
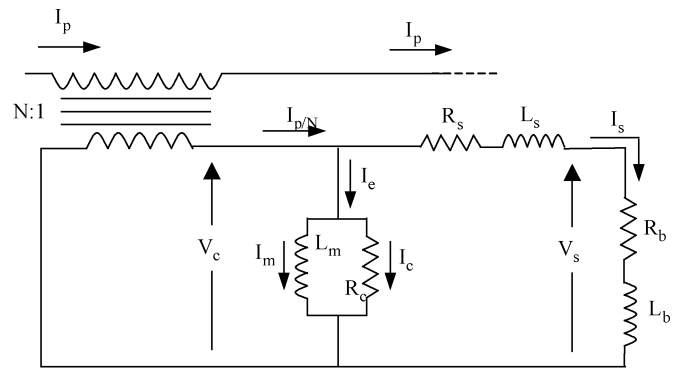


Fig. 4. Online CT saturation compensation process.

and outputs the received sample to the output control module. The system then uses the received sample plus previously saved samples to determine if they meet a predefined set RP criterion. After an RP detected, for each received current data sample, the system determines whether the received data sample is within unsaturated waveform portion or saturated waveform portion. Data samples within saturated waveform portions will be replaced with compensated samples. Further, after storing the received sample, either as the received sample or as the compensated sample, the system determines if a reset RP criterion has been met. Reset RP criteria may be based on a predefined time delay or by checking the current magnitudes of samples, and the like. The system resumes obtaining another received sample after finishing the above process and repeats the same procedure for every newly received sample.

IV. PERFORMANCE EVALUATION

A wide range of test cases was established and analyzed to demonstrate the performance of saturation compensation. In these test cases, the fault current waveforms were obtained from EMTP simulations based on realistic subtransmission network parameters, representing various fault conditions in terms of short-circuit levels, fault inception angles, and primary time constants. The CT modeling and compensation algorithm were implemented in the MATLAB platform. Fig. 5 shows the CT model used in this study with all of the quantities referred to the secondary side. The CT ratio used in the test cases is 1000/5. The accuracy of CT modeling in MATLAB platform was verified against EMTP built-in modeling features. The preference of using the MATLAB-based modeling approach over the direct application of EMTP built-in models is mainly to provide desired program modeling flexibility and testing process efficiency with regard to variations of CT saturation and secondary parameters. The performance of compensation algorithm can be illustrated conceptually by the following representative test results. These test cases (Case 1 through



I_p = Primary current
 I_p/N = Ideal secondary current
 I_s = Secondary current
 I_e = Exciting current
 I_c = Core eddy loss current
 I_m = Magnetizing current
 L_m = Magnetizing inductance, $L_m = \lambda_m / I_m$
 λ_m = Magnetizing flux
 N = CT turns ratio
 R_c = Core loss resistance
 R_s = Secondary resistance
 R_b = Burden resistance
 L_s = Secondary Inductance
 L_b = Burden Inductance

Fig. 5. CT equivalent circuit diagram.

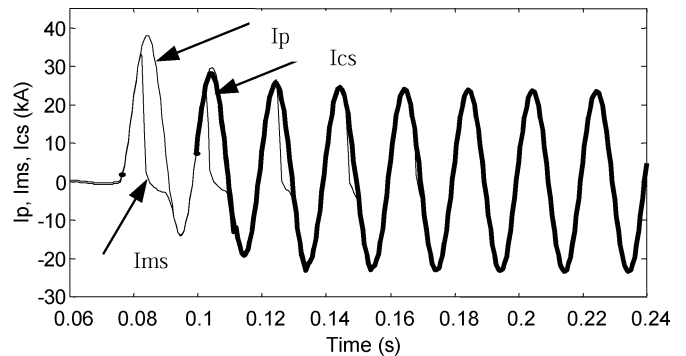


Fig. 6. Results of Case 1.

Case 3) were simulated at the same location of test network but with varying fault conditions or CT secondary parameters:

	Fault inception angle (in degrees)	CT secondary loading (100 VA)
Case 1 :	0	pure resistive
Case 2 :	0	0.5 power factor
Case 3 :	135	pure resistive

Figs. 6–8 show the test results. The results of each test case are presented with three fault current waveforms: the primary fault current waveform I_p , which is simulated using EMTP under given fault conditions; the measured secondary fault current waveform I_{ms} , which is a partially distorted fault current waveform due to CT saturation effects; and the compensated secondary fault current waveform I_{cs} , which is a reconstructed version of the measured secondary fault current waveform. In this paper, we formulated the compensation algorithm with data samples in two consecutive unsaturated waveform portions. As such, the compensation algorithm will be enabled no longer than one-and-a-half cycles after fault initiation. This means accurate current measurements can be expected within about 25 ms after fault initiation.

Quantitative evaluation was performed based on the measured rms values from simulated fault current waveforms, where

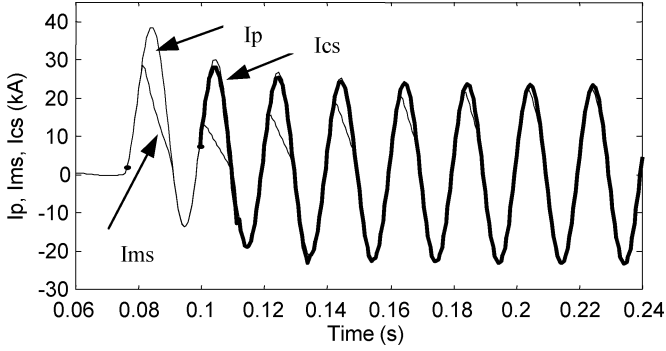


Fig. 7. Results of Case 2.

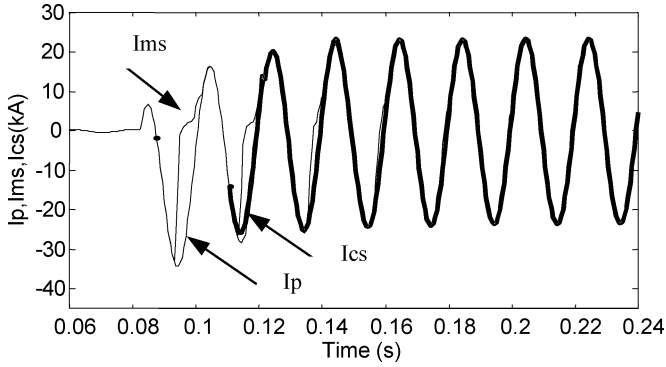


Fig. 8. Results of Case 3.

the CT model used reflects typical saturation characteristics. This means the performance of CT will be satisfactory for carrying steady-state and symmetrical currents up to 20 times the rated current at rated secondary burden. However, it is well known that faults in power systems very often involve dc offset superimposed on the symmetrical component in one or more of the three-phase currents, resulting in CT saturation at much lower current levels than symmetrical currents without dc offset.

The test results presented in this paper are based on 320 test cases, each representing a specific combination of the following assumptions:

Short-circuit current	5/10/15/20 kA
Inception angle	0/45/90/135 degree
Primary time constant	30/40/50/60/70 ms
Secondary loading	50/100 VA
Burden power factor	1.0/0.5.

The rms value of fault current waveform is calculated as

$$rms = \sqrt{\left(\frac{1}{N} \sum_{n=1}^N i(n)^2\right)} \quad (7)$$

where $N = 32$ (i.e., the sampling rate used in the simulation). Fig. 9 shows an example of calculated rms values based on measured fault current waveforms.

Since the true rms values of steady-state fault current waveforms are known from test case assumptions, the following error indices (EI) can be computed:

$$EI_{com} = \max \left\{ \frac{(rms_{true} - rms_{com})}{rms_{true}} \right\} \times 100\% \quad (8)$$

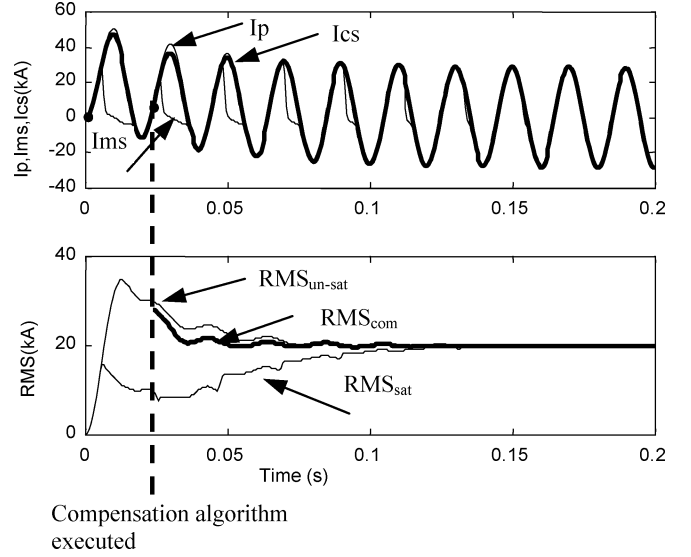


Fig. 9. Comparison of calculated rms values.

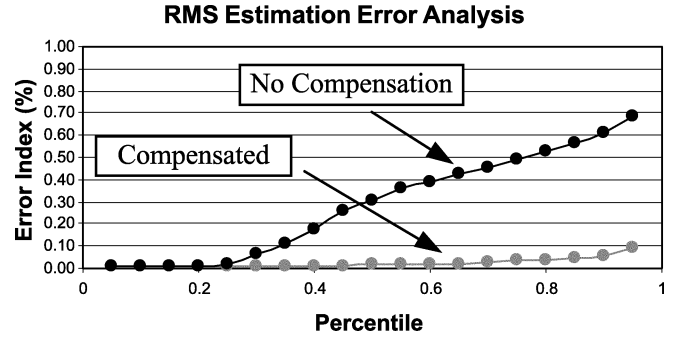


Fig. 10. RMS estimation error analysis.

$$EI_{sat} = \max \left\{ \frac{(rms_{true} - rms_{sat})}{rms_{true}} \right\} \times 100\% \quad (9)$$

where rms_{com} and rms_{sat} refer to the measured rms values from compensated and saturated fault current waveform portions. In Fig. 9, the compensated data samples during the first cycle are actually obtained after the compensation algorithm is executed. These compensated data samples are needed for accurate rms calculation during the cycle immediately after enabling compensation algorithm.

Equation (8) or (9) basically calculates, point by point, the difference between rms_{true} and rms_{com} or between rms_{true} and rms_{sat} and then determines the maximum error of underestimated rms values. As mentioned earlier, underestimation of rms values is the primary concern of overcurrent protection relays. Apparently, the closer the index is to 0, the less significant the error is in rms estimation.

The overall performance of compensation algorithm on the 320 test cases can be examined by percentile analysis of rms estimation errors as shown in Fig. 10. From Fig. 10, it can be seen that the compensation algorithm effectively controls the rms errors to less than 10% for 95% of the test cases. The maximum rms error is 14.94%, which corresponds to a test case assuming a short-circuit current 20 times the rated CT current, 70 ms of primary time constant, and a secondary burden 2 times the IEEE standard loading (i.e., 100 VA at 0.5 power factor).

TABLE I
STATISTICAL ANALYSIS OF RMS ESTIMATION ERRORS

Assumption	Cases	Max	Mean	Median	95% Percentile	
CT Parameters	R50	80	13.06%	1.83%	0.92%	5.93%
	IEEE50	80	10.81%	2.20%	1.62%	5.58%
	R100	80	13.74%	3.09%	0.98%	12.07%
	IEEE100	80	14.94%	3.36%	2.20%	10.68%
Primary Time Constant (ms)	30	64	13.74%	3.76%	3.42%	11.35%
	40	64	12.07%	2.24%	1.50%	7.64%
	50	64	10.98%	1.99%	1.18%	6.96%
	60	64	11.86%	2.26%	1.08%	7.84%
	70	64	14.94%	2.86%	1.03%	11.89%
Short Circuit Current (kA)	5	80	13.68%	2.92%	1.59%	10.92%
	10	80	13.74%	2.54%	1.36%	9.05%
	15	80	12.79%	2.40%	1.25%	8.97%
	20	80	14.94%	2.62%	1.49%	7.48%
Inception Angle (degree)	0	80	13.74%	4.70%	3.58%	12.15%
	45	80	14.94%	3.12%	1.97%	10.67%
	90	80	4.87%	1.23%	1.06%	2.82%
	135	80	4.06%	1.44%	1.20%	3.35%

Table I provides more detailed statistical analysis of rms estimation errors, where R50 and R100 represent the test cases assuming pure resistive burden at 50 and 100 W, and IEEE50 and IEEE100 represent the test cases using IEEE standard burden at 50 and 100 VA.

It can be observed from the above statistical analysis that the algorithm performance is reliable for a wide range of variations in fault conditions and CT parameters. The rms estimation errors caused by CT saturation effects can be controlled within or very close to 10% of true rms values for 95% of the test cases under various case grouping categories. Statistical analysis also indicates that the primary time constant (i.e., the composite value of line and source time constants) is an important factor affecting the performance of the compensation algorithm. However, as the primary time constants associated with subtransmission networks typically range from 40 to 60 ms, satisfactory algorithm performance can be expected. For the test cases representing rated CT secondary burden and typical primary time constants (a total of 96 cases under this category), the maximum rms error is 7.79% and the rms error for 95% percentile is 5.22%. Further tests have shown that the compensation accuracy will not be affected when there is a skew of reference points as long as it is detected and set within about 30° after fault initiation.

V. CONCLUSION

This work presents an effective and practical solution for on-line CT saturation compensation. The introduced compensation

method is capable of providing reliable input signals to power system protection and control devices/apparatus that require accurate current measurements. Extensive test cases have shown that the introduced compensation method is robust to various fault conditions and CT characteristics.

REFERENCES

- [1] Y. C. Kang, J. K. Park, S. H. Kang, A. T. Johns, and R. K. Aggarwal, "An algorithm for compensating secondary current of current transformers," *IEEE Trans. Power Delivery*, vol. 12, pp. 116–124, Jan. 1997.
- [2] D. C. Yu, Z. Wang, J. C. Cummins, H.-J. Yoon, L. A. Kojovic, and D. Stone, "Neural network for current transformer saturation correction," in *Proc. IEEE Transm. Distrib. Conf.*, New Orleans, LA, Apr. 1999.
- [3] B. Kasztenny, E. Rosolowski, M. Lukowicz, and J. Izykowski, "Current related relaying algorithms immune to saturation of current transformers," in *Proc. Conf. Developments in Power System Protection*, Mar. 1997.
- [4] T. Bunyagul, P. Crossley, and P. Gale, "Overcurrent protection using signals derived from saturated measurement CTs," in *Proc. IEEE Summer Meeting*, Vancouver, BC, Canada, July 2001.
- [5] K. Vu and A. Khan, "Waveform Reconstruction From Distorted (Saturated) Currents," U.S. Patent (# 5 974 361), Oct. 1999.
- [6] *IEEE Standard Requirements for Instrument Transformers*, IEEE Std. C57.13-1993.

Jiuping Pan (M'97) received the B.S. and M.S. degrees in electric power engineering from Shandong University, Jinan, China, and the Ph.D. degree in electrical engineering from Virginia Polytechnic Institute and State University, Blacksburg.

Currently, he is a Principal Consulting R&D Engineer of ABB Corporate Research, Raleigh, NC. His research interests include power system planning, security analysis and control, network asset management, and market simulation studies.

Khoi Vu (M'95) received the B.S., M.S., and Ph.D. degrees in electrical engineering from the University of Washington, Seattle.

Currently, he is an Executive Consulting R&D engineer with ABB Corporate Research, Raleigh, NC. His research interests are power system control and energy markets.

Yi Hu (M'00) received the B.S. and M.S. degrees in electrical engineering from the Southeast University and the Nanjing Automation Research Institute, Nanjing, China, respectively.

He received the Ph.D. degree in electrical engineering from the University of Manitoba, Winnipeg, MB, Canada. His research interests are power system control and protections, signal processing, communication systems, and embedded systems.